Biosensors and Bioelectronics 126 (2019) 230–239

Contents lists available at ScienceDirect

Biosensors and Bioelectronics

journal homepage: www.elsevier.com/locate/bios

Electrochemical immunosensor for CDH22 biomarker based on benzaldehyde substituted poly(phosphazene) modified disposable ITO electrode: A new fabrication strategy for biosensors

Muhammet Aydın[a], Elif Burcu Aydın[a,*], Mustafa Kemal Sezgintürk[b]

[a] Tekirdag Namık Kemal University, Scientific and Technological Research Center, Tekirdağ, Turkey
[b] Çanakkale Onsekiz Mart University, Faculty of Engineering, Bioengineering Department, Çanakkale, Turkey

ARTICLE INFO

Keywords:
Benzaldehyde substituted poly(phosphazene)
Cadherin-like protein 22
Electrochemical impedance spectroscopy
Cancer biomarker

ABSTRACT

A novel label-free impedimetric immunosensor was fabricated for rapid, selective and sensitive detection and quantification of Cadherin-like protein 22 (CDH22), a cancer marker, in human serum by using easy and quickly prepared disposable ITO immunoelectrode. cancer marker, in human serum by using easy and quickly prepared disposable ITO immunoelectrode. The biosensing approach implied the use of ITO electrode coated with poly (phosphazene) polymer including benzaldehyde groups attached with CDH22 antibody and CDH22 antigens. Benzaldehyde side groups containing poly(phosphazene) film coated disposable ITO electrode were utilized as an immunosensing platform and anti-CDH22 antibodies bound to aldehyde groups of benzaldehyde substituted poly(phosphazene) (P-PHP) covalently. The immunosensor modification steps and affinity interaction between anti-CDH22 antibodies and CDH22 antigens were observed by EIS and CV in the presence of the redox couple. Furthermore, antibody immobilization was followed via FTIR and Raman spectroscopy. The morphological analyses of the suggested immunosensor during the fabrication steps were carried out with SEM and AFM monitoring. All the experimental parameters affecting the construction of the immunoelectrodes were optimized. The fabricated immunosensor exhibited an excellent working performance with a wide detection linear range (0.015–2.9 pg/mL) and low limit of detection (4.4 fg/mL). Moreover, the proposed immunosensor had great reproducibility, repeatability and long-term stability. Additionally, the fabricated immunosensor was successfully used in the quantification of CDH22 in human serum without any pretreatment.

1. Introduction

Cancer is a group of diseases including abnormal cell growth and division in an uncontrolled way. Some cancers may eventually spread into other tissues (Karimi-Maleh et al., 2017). Cancer starts when a gene changes form in one cell or a few cells, then it begins to grow and multiply too much. When cancer is not diagnosed early, it causes death. Therefore, the early diagnosis of cancer is important in human health (Amani et al., 2018). Biomarkers are biological molecules found in blood and other body fluids, which are signs of normal or abnormal biological states or conditions. They are released from tumor tissue, and are significant signs for cancer detection (Amani et al., 2018; Aydın et al., 2018a; Rauf et al., 2018). To diagnose cancer early, a sensitive and rapid method is required. A lot of different techniques are already used for measurement of biomarkers in human serum and other body fluids. In clinical analysis, Enzyme-linked Immunoassay (ELISA), radio immunoassay and fluorescence immunoassay methods are usually utilized for biomarker measurement in serum. The classic enzyme–linked immunosorbent assay (ELISA) is one of the most widely used methods for determination of biomarkers in biological fluids based on spectrophotometric reading. ELISA provides highly reproducible, sensitive and specific, quantitative data that makes it an advantageous tool in scientific research and clinical diagnosis. However, it suffers the drawbacks of time–consuming activity due to the long and tedious assay procedure, the short shelf life of the labeled antibody, excess reagent consumption, high cost and the narrow dynamic range (Zhou et al., 2015). Moreover, the detection limit of conventional ELISA is barely less than the nanomolar concentration level, which is inadequate to reach the clinical threshold of many protein biomarkers, especially in the early stage of diseases (Arya and Estrela, 2018). In contrast to immunoassays, in immunosensors the same receptor surface can be reused for many measurements. The antibody layer is largely secured during

* Corresponding author.
E-mail address: ebbahadir@nku.edu.tr (E.B. Aydın).

https://doi.org/10.1016/j.bios.2018.10.051
Received 29 August 2018; Received in revised form 23 October 2018; Accepted 24 October 2018
Available online 02 November 2018
0956-5663/

sensor reuse, which provides an economic advantage of the immunosensor compared to commercial kit assays like ELISA. The reusability is a remarkable property of immunosensor. After measurement of antigens, the regeneration of the used immunosensor is performed by dipping in basic solution (NaOH/NaCl) or glycine/HCl buffer solution (pH 2–3) for few min, and then by washing with distilled water several times to desorb the binding antigens. Direct signal generation potentially enables real-time monitoring of analytes, thus making immunosensors suitable tools for continuous monitoring (Bojorge Ramírez et al., 2009). To overcome these drawbacks, alternative methods are developed (Amani et al., 2018; Aydın et al., 2018a). Electrochemical immunosensor is a promising candidate for biomarkers detection (Bahadır and Sezgintürk, 2015). It has been intensively studied for its high sensitivity, low cost, excellent detection limits, fast response, ease of handling and miniaturization (Zhou et al., 2015).

Cadherin-like protein 22 (CDH22), which is known as PB-cadherin (Zhou et al., 2009), is a transmembrane glycoprotein and present in cell-cell adhesion and metastasis. CDH22 hypermethylation is an independent prognostic biomarker in breast cancer (Martín-Sánchez et al., 2017; Piche et al., 2011). In addition, it is a member of cadherin superfamily. It is highly expressed in the pituitary gland and brain. It has a role in tissue formation in neural and nonneural cells of the brain and neuroendocrine organs (Zhou et al., 2009). Over-expression of CDH22 causes colorectal cancer (Martín-Sánchez et al., 2017; Piche et al., 2011; Zhou et al., 2009), breast cancer (Martín-Sánchez et al., 2017) and metastatic melanoma (Piche et al., 2011). As reported Kelly et al. (2018), Cadherin-22 is a powerful prognostic marker for advanced cancer stages and patient outcomes. It is a cell–cell adhesion molecule and a potential factor in cancer metastasis, or spread, and showed that hindering it decreases the adhesion and invasion rate of breast and brain cancer cells. Therefore, this biomarker is important than other biomarkers that used in diagnosis of breast cancer (Kelly et al., 2018). The determination of CDH22 biomarker is usually performed by using ELISA kit. The linear range and detection limit of the ELISA kit are 15.6–500 ng/mL and 2 ng/mL, respectively (www.mybiosource.com). However, immunosensors for the CDH 22 biomarker determination are not available in the literature.

Electrochemical biosensors are popular in cancer biomarker detection due to their excellent sensitivity, specificity, and reproducibility. These biosensors are based on the selective interaction between the target analyte and biorecognition molecule to form an electrical signal that is related to the analyte concentration being studied. They can work on different detection strategies including amperometry, potentiometry, conductometry, voltammetry and electrochemical impedance spectroscopy (EIS). Electrochemical impedance spectroscopy (EIS) is a very promising biosensing detection method and provides very low detection limit (Karimi-Maleh et al., 2013, 2014). A typical EIS biosensor includes a sensing element captured on the conducting surface and this sensing element interacts with the target protein of interest. Label free electrochemical immunosensors provide a lot of benefits such as ease of use, fast response, low cost and the ability to directly monitor the changes in the signals originated from the specific binding reaction between antibody and antigen without the need for any labels (Amani et al., 2018; Aydın et al., 2018b). Moreover, immunosensors are generally ultrasensitive devices, but the fabrication steps affect the sensitivity of immunosensors (Aydın et al., 2018b; Khashayar et al., 2017). The fabrication protocols of label-free electrochemical immunosensors are simple and low cost. Label-free strategies reduce the number of immobilization stages (Aydın and Sezgintürk, 2018; Ferreira and Sales, 2014). In biosensing system, electrode fabrication procedure has an important role in the success of biosensor. Therefore, different strategies such as adsorption, electrophoretic deposition, electrochemical deposition have been utilized for biosensor construction. These strategies provide stable and long-life biosensor (Aydın and Sezgintürk, 2017). Spin-coating is another biosensing electrode construction method. This method is a simple and easy way for forming uniform thin film on the platform. A drop of fluid is settled on the center of the platform and then the platform is spun at high speed. In this way, the fluid spreads over the platform forming a thin film. Moreover, it provides reproducible films on the platforms (Aydın et al., 2018a; Ghayedi Karimi et al., 2018). Although spin coating is a simple method, it is rarely used. A great deal of attention has been directed towards the application of polymers in sensor and biosensor systems. The construction of electrochemical biosensors based on polymer has become a popular application in electrochemical researches. Polyphosphazenes are inorganic polymers which have an inorganic backbone. They include nitrogen and phosphorus atoms and they are the most studied phosphorus nitrogen compounds. These polymers are versatile because various substituents can attach to the backbone phosphorus atom. Thus, the resulting polymer has excellent features and is convenient for many potential applications, including biomedical researches and drug delivery examinations (Kumar et al., 2015). These polymers have antimicrobial and biological activities on bacterial and yeast cells. Depending on the side groups of polyphosphazenes, they can be biodegradable. This property is important for tissue engineering applications (Pamukçi et al., 2007). The synthesis process of this polymer had long steps, but polyphosphazenes with a backbone of alternating phosphorus and nitrogen atoms two organic side groups provided an ideal immobilization matrix in biosensor development (Sohn and Jun, 2009). The key feature of polyphosphazene chemistry allowed easy introduction of two functional groups in a repeating unit, which were still largely uncommon in macromolecular chemistry. Unlike many other classes of synthetic polymers, polyphosphazenes offered an easy addition of functional side groups to the backbone (Allcock, 1998). These advantages were important to immobilization of biorecognation elements to the electrode surface.

The novelty of this study is the construction of an ultra-sensitive label-free impedimetric immunosensor based on benzaldehyde substituted poly(phosphazene) modified disposable ITO electrode for CDH22 determination. For the first time, benzaldehyde side groups containing poly(phosphazene) were synthesized to form antibody immobilization platform and used to fabricate the biosensor for CDH22 determination. In this study, aldehyde groups of polymer were bound to amino groups of antibody without using a crosslinking agent. Therefore, this polymer was utilized as immobilization matrix because of its direct binding property. In addition, the advantages of this study involve effective and easy bonding formation due to aldehyde groups of poly(phosphazene) and rapid and simple electrode fabrication using spin-coating method. The study focused on the EIS technique to determine CDH22 in human serum samples. All experimental parameters such as concentrations of polymer, and incubation times of antibody and antigen were studied and optimized to obtain high reproducibility, repeatability and sensitivity of the analysis. Additionally, the accuracy of the EIS method was tested by means of standard addition technique.

2. Experimental

2.1. Reagents and materials

Phosphonitrilic chloride trimer ($P_3N_3Cl_6$, Sigma-Aldrich, 97%), 4-hydroxybenzaldehyde (Sigma-Aldrich, 98%), Triethylamine (TEA, Sigma-Aldrich, ≥ 99%), Aluminum Chloride ($AlCl_3$, Sigma-Aldrich, 99%) and Sodium metal rod (Sigma-Aldrich) were used as purchased without further purification. Tetrahydrofuran (Sigma-Aldrich, anhydrous, ≥ 99.9%), Acetone (Sigma-Aldrich, HPLC Plus, ≥ 99.9%), Chloroform, (Sigma-Aldrich, dried (max. 0.003% H_2O)), Methanol (Sigma-Aldrich, for HPLC, ≥ 99.9%) and Hexane (Sigma-Aldrich, anhydrous, 95%) were used for synthesis or purification steps. Potassium ferro- and ferricyanide, KCl, KH_2PO_4, K_2HPO_4 were purchased from Sigma-Aldrich. Sulfuric acid and hydrochloric acid were ACS grade and purchased from Across. Clear glass prescored ampoules (10 mL × 108 mm) were obtained from Wheaton® scientific company.

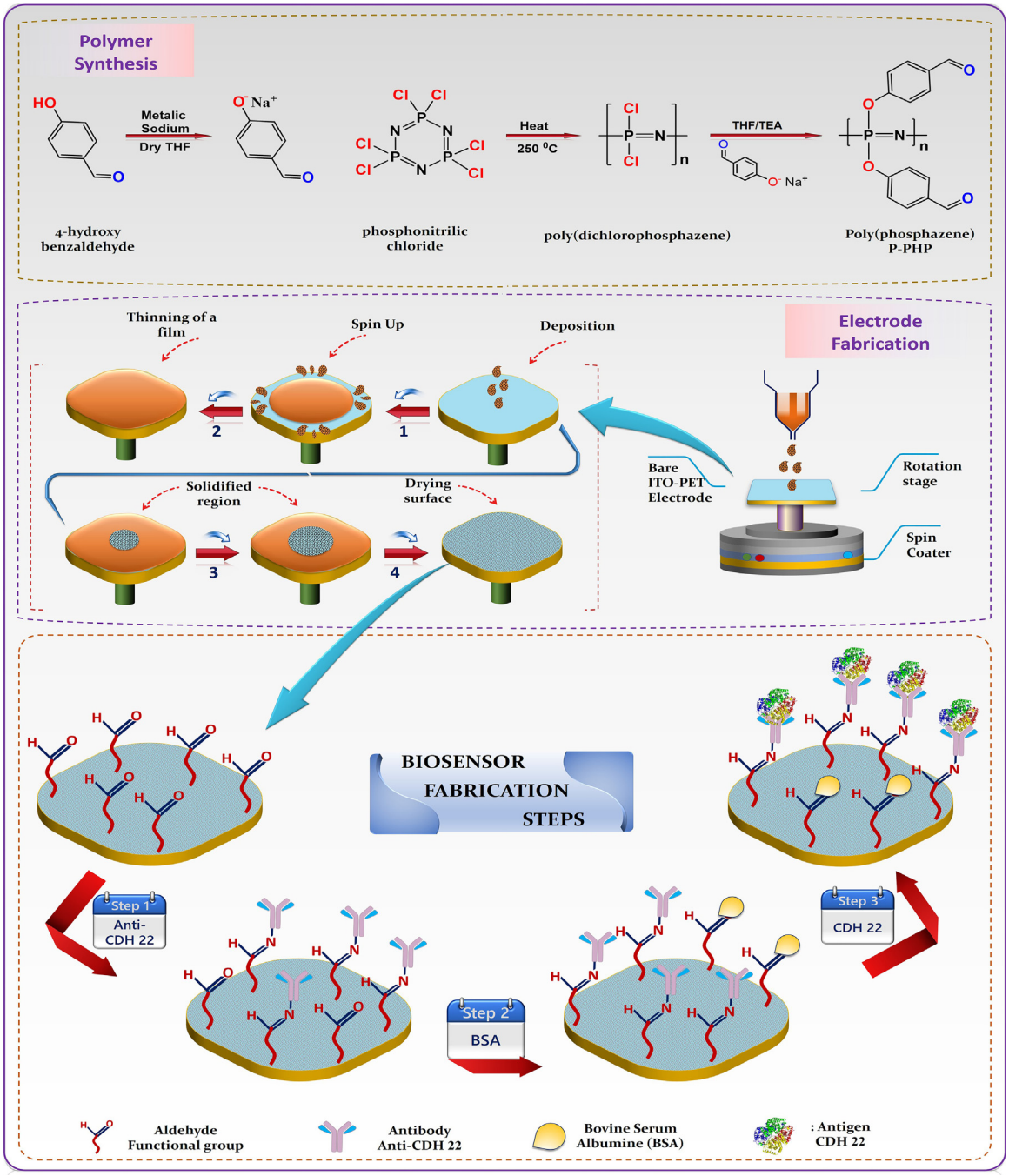

Scheme 1. (A) The synthesis process for benzaldehyde substituted poly(phosphazene) and (B) the fabricating stage of the immunosensor.

Indium tin oxide (ITO) electrodes (5 mm × 20 mm, 60 Ω/cm^2), Monoclonal Anti-CDH22 antibody, and CDH22 human recombinant were purchased from Sigma-Aldrich. Anti-CDH22 antibody, recombinant human CDH22 and BSA solutions were prepared utilizing phosphate buffer (PBS 50 mM, pH 7.4) and stored at −20 °C. Ferri-ferro solution contained 1 M KCl, 5 mM $[Fe(CN)_6]^{-4}$ and 5 mM $[Fe(CN)_6]^{-3}$ in PBS and was employed as redox couple. Interleukin1α (IL-1α), interleukin-1β (IL-1β), tumor necrosis factor α (TNF α), interleukin 8 (IL 8), receptor activated kinase 1 (RACK1) and Sex determining region Y-box 2 (SOX 2) were utilized as potential interference molecules to investigate the selectivity of the proposed immunosensor.

2.2. Measurement

Electrochemical measurements (CV and EIS) were carried out using a Gamry Potentiostat/Galvanostat Reference 1000 equipped with Gamry Analyst Software. The electrodes utilized in the electrochemical system were an ITO working electrode (2*20 mm), a platinum counter electrode, and an Ag/AgCl reference electrode. The reference and counter electrodes were obtained from BASi Company. CV measurements were performed in a potential range from 0 to 500 mV at a scan rate 100 mV/s. EIS measurements were carried out at 50,000 Hz and 0.05 Hz for initial and final frequency, respectively. Proton nuclear magnetic resonance (1H NMR) spectra were recorded on a 400 MHz Bruker Avance II. Attenuated Total Reflection Fourier Transform Infrared (ATR-FTIR) measurements were performed using a Bruker

Company Vertex 70 FTIR infrared spectrometer in the range of 4000–400 cm^{-1} at room temperature and the obtained data were employed without any corrections. Dispersive Raman measurements were carried out with a Thermo Company DXR Raman spectrometer including a 780-nm excitation laser and a confocal microscope with 5 objectives. Raman spectra were recorded using the Thermo Scientific OMNIC™ Software with Array Automation function. The morphological analyses of benzaldehyde polymer modified ITO electrodes were performed utilizing SEM and energy dispersive X-ray (EDX) studies. SEM images were obtained using Field Emission scanning electron microscope (QUANTA FEG-250) with low vacuum detector (LFD). AFM İmages were taken using a AFM PLUS+, NanoMagnetic Instrument. The electrodes scans were recorded under ambient conditions with an isolated air table. The device was operated in tapping AFM mode. The scan rate was 5 μm/s with a resolution of 256 pixels per line. Three-dimensional (3D) AFM images were generated using Nanomagnetics image analyzer software.

2.3. Procedures

2.3.1. Synthesis of polymer

Synthesis of benzaldehyde substituted poly(phosphazene) was a two-step reaction sequence. The first stage contained the preparation of poly(dichlorophosphazene), and the second required the replacement of the chlorine atoms in polymer by reactions with deprotened of 4-hydroxybenzaldehyde (Sohn et al., 1995). The most widely used method for preparing poly(dichlorophosphazene) was the thermal ring-opening polymerization. However, thermal ring opening polymerization did not allow for precise control over molecular weight or polymer chain length distribution. Moreover, many factors such as purity of chemicals, presence of water for cleaning of glassware etc. affected the ring-opening polymerization (Allcock, 1992). Therefore, we had to take several measures to eliminate the impact of such factors. Prescored clear glass ampoules (10 mL) were soaked in acidic solution and washed with ultra-pure water several times and then dried at 125 °C in the laboratory oven. The clean and dried ampoules were taken to a portable desiccator and then moved to an argon-loaded glovebox. The cooled ampoule in the glovebox was loaded with phosphonitrilic chloride trimer 1 gr (2.87 mmol) and aluminum chloride 19.2 mg (~ 5%, 0.143 mmol) as catalyst and attached to a vacuum line. Then, it was taken out from the glovebox. The ampoule was evacuated and sealed with a flame. The polymerization reaction was carried out directly at 250 °C in the oven for 24 h. The polymer reaction was stopped before cross-linking, in other words, before returning to excessively viscous, because cross-linking tends to occur when the polymer ampoule is overexposed to heat. The slices of Sodium metal were suspended in dry THF (5 mL) in a three-neck-flask equipped with magnetic stirring bar under dry argon purge and a solution of 4-hydroxybenzaldehyde (2.1 g, 20 mmol) in THF (10 mL) was added dropwise through a dropping funnel. The reaction mixture was stirred for 6 h at room temperature and dry-preserved for further use. After polymerization, sealed ampoule was opened in the glovebox and 10 mL dry THF was added. The polymer solutions were added to Na salt of benzaldehyde solution and stirred for 48 h in the glovebox and then precipitated twice in petroleum ether. Yellow colored polymer was recuperated by vacuum filtration and dried under reduced pressure at 30 °C (Scheme 1).

FT-IR (ATR, cm^{-1}): 2830 (-CH_2); 1700 (C=O); 1595, 1501(aromatic); 1191 (P=N); 1152 (P-O-C); 920 (P-O-Ph); 828. Raman (λ_{laser} = 780 nm, cm^{-1}): 3073, 3000; 1696 (C=O); 1598, 1509 (aromatic); 1233, 1159 (P=N); 1010 (P-O-Ph); 738(PN). ^{1}H NMR ($CDCl_3$, 400 MHz) δ: 7,19 ppm (Ha; 4H, *ortho*); 7,48 ppm (Hb; 4H, *meta*); and 9,66 ppm (Hc; 1H, *CHO*). ^{31}P NMR (DMSO-D_6, 202.4 MHz): −5.3 ppm.

2.3.2. Construction of the immunosensor

The fabrication process of the proposed immunosensor is shown in Scheme 1. First, the surface of ITO electrode was cleaned in acetone, soap solution and ultra-pure water by using ultrasonic bath. Second, 30 μl P-PHP polymer solved in NMP/Acetone solvents (1:2, v/v) was spread over the ITO electrode surface. Finally, it was spun at 1000 rpm and maintained there for sixty seconds to remove the solvent. Spin-coating method, one of the cheapest and effective coating method, is widely used in the fabrication of sensor and in many applications. Then, the prepared electrode was dipped in PBS solution containing anti-CDH22 antibody. The immunosensor was washed with ultra-pure water to remove unbound antibodies. Subsequently, 0.5% BSA (w/v) prepared in 50 mM PBS buffer (pH 7.4) was utilized to block aldehyde groups on the electrode surface. In this way, non-specific adsorptions were avoided. After 60 min incubation at room temperature and then rinsing with ultra-pure water, the immunosensor was ready to measure the CDH22 antigen.

2.3.3. Determination of CDH22 with the proposed immunosensor

The determination of CDH22 was carried out by immersing the immunosensor 5 mM $Fe(CN)_6^{3-/4-}$ solution prepared in 1 M KCl and measuring impedance between 0.5 and 50,000 Hz. The change in impedance was utilized for CDH22 quantification.

2.3.4. Validation and statistical evaluation of the study

To investigate of the accuracy and precision of the immunosensor, the parameters of limit of detection (LOD), limit of quantification (LOQ), linear detection range, repeatability, reproducibility and selectivity were studied. For linear detection range investigation, the increase in impedance with increasing CDH22 concentration was monitored and the relationship between CDH22 concentration and impedance was used for determination in linear detection range. LOD and LOQ of the developed immunosensor were calculated according to IUPAC recommendations $3S_b/b$ and $10S_b/b$, where S_b is the standard deviation (n = 10) of the blanks, and b is the slope of the calibration curve. Repeatability of the proposed immunosensor was also investigated by determination of CDH22 (0.35 pg/mL). The reproducibility of the immunosensor was also examined by recording the EIS responses of ten individual immunosensors. To evaluate the selectivity of the constructed CDH22 immunosensor, the influence of several interfering agents such as IL-1β, IL-8, TNF-α, IL-1α, SOX2 and RACK 1 on the determination of CDH22 under the optimal experimental conditions was investigated.

Statistical evaluation of the study was performed by calculation of relative standard deviation (RSD) of the obtained results. In repeatability study, CDH 22 antigen solution which was at same concentration was measured by using 20 equally prepared immunosensors. In reproducibility study, 10 different immunosensors that were prepared under the same conditions were investigated by measuring different concentration of CDH22 antigens. Moreover, statistical analyses were performed by utilizing PASW Statistic 18 program. One Sample T Test was chosen as a test method and this test was carried out at a 95% confidence interval. Apart from One Sample T Test, ANOVA test was performed.

2.3.5. Human serum samples analysis

Human serum samples were obtained from the NKU hospital of Tekirdağ. These samples were studied with the proposed immunosensor after a 10,000 fold dilution with phosphate buffer (50 mM, pH 7.4). The accuracy of measurement was tested by means of standard addition method.

3. Results and discussion

3.1. Chemical characterization of the immunosensor

Synthesis of benzaldehyde substituted poly(phosphazene)(P-PHP) included ring opening polymerization and replacement reactions. These reaction steps are illustrated in Scheme 1.

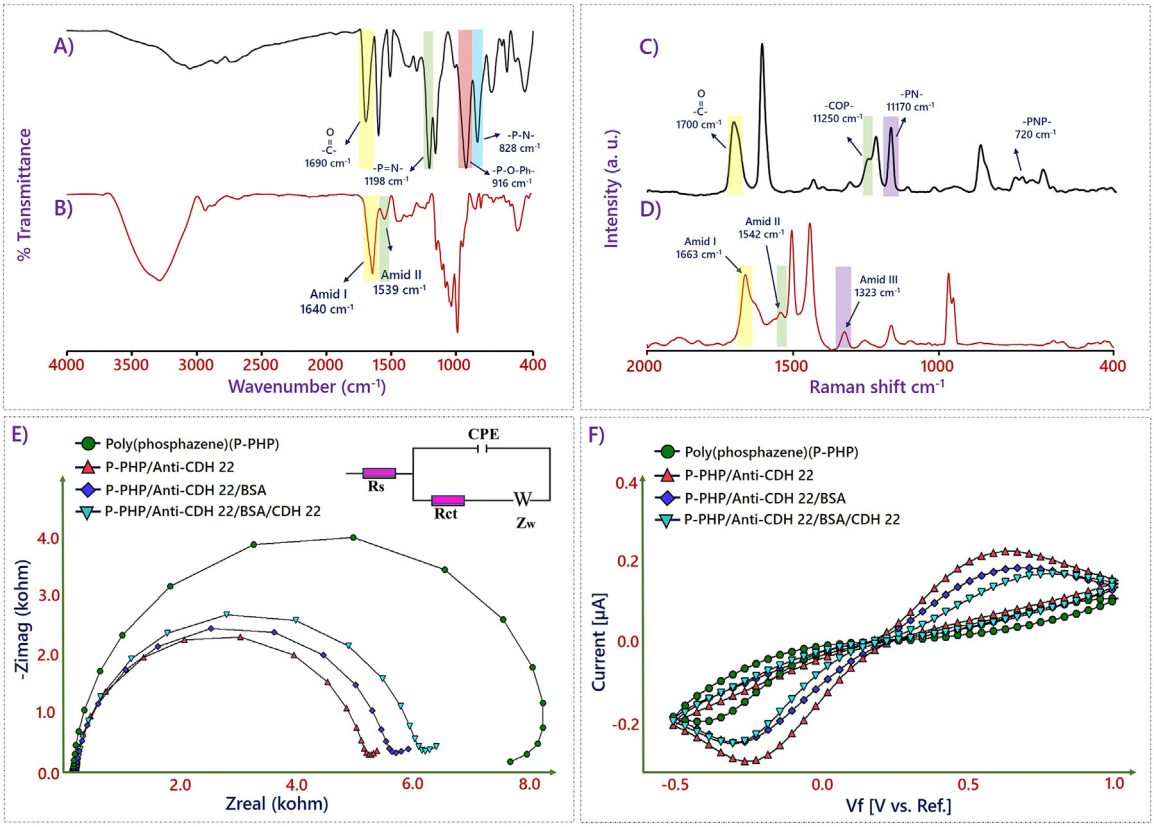

Fig. 1. FTIR and Raman spectra of benzaldehyde substituted poly(phosphazene) (A and C) and anti-CDH22 antibody modified ITO electrode (B and D), Nyquist plots (E) and cyclic voltammograms (F) recorded at modified ITO electrode. Inset of 1E: Equivalent circuit applied to fit impedance measurements.

The chemical structure of (P-PHP) was characterized by several spectral techniques (FTIR, DXR-RAMAN, ^{1}H NMR and ^{31}P NMR) to illustrate the success of the synthesis way of the (P-PHP) and spectral results were shown in detail in the Supplementary material file (Fig. SI-1, Fig. SI-2, Fig. SI-3 and Fig. SI-4). The chemical bonding between poly (phosphazene) coated ITO electrode surface and anti-CDH 22 antibody was investigated by means of FTIR and RAMAN spectrometry. The FTIR spectra of polymer (P-PHP) layer obtained after formation on ITO surface (black line) and immobilization of anti-CDH 22 antibody on the polymer (P-PHP) modified ITO electrode surface (red line) are illustrated in Figs. 1A and 1B, respectively. As seen in Fig. 1A, the aldehyde substituted poly(phosphazene) modified ITO surface had the two absorption peaks at 1198 cm^{-1} and 828 cm^{-1} that showed the presence of P = N and P-N bounds in polymer P-PHP (Carriedo et al., 1998; Fiedler et al., 2018; Luther et al., 2003). The strong signal seen around 1690 cm^{-1} was attributed to C=O stretching vibration of aldehyde side groups in polymer (Aydın et al., 2018a). Besides, the peak around at 916 cm^{-1} was attributed to P-O-Ph stretching vibration of side groups (Allcock et al., 1966; Jiang et al., 2015). The major functional group vibrational signals of a protein structures are -NH and -OH bands (3000–3700 cm^{-1}) and amide I, II, III bands across the fingerprint region 1700–500 cm^{-1} (Tranter, 2017). At red line in Fig. 1B, there were broad and intense bands for amide I at ~ 1640 cm^{-1} and for amide II at ~ 1539 cm^{-1}, and this clearly indicated the binding of the anti-CDH22 to polymer P-PHP (Aydın et al., 2018a; Banas et al., 2015). The chemical structure of P-PHP modified ITO sheet and anti-CDH 22 antibody immobilized ITO sheet was investigated via Raman spectral technique (Figs. 1C and 1D). The chemical structure of polymer and the molecular structure of proteins are usually monitored via Raman spectroscopy (Aydın et al., 2018b; Chen and Lord, 1974).

Raman spectral technique is complementary to FTIR spectroscopy in that they both probe the vibrations of molecules, but from different perspectives (Alula et al., 2018). The Raman spectra illustrated that the -PNP- and -PN- bonding stretching vibrations of poly(phosphazene) backbone were seen at 720 cm^{-1} and 1170 cm^{-1}. Raman spectroscopy was used to prove amide bonds present in molecular structure. The bands of amide I, II and III regions are seen between 1650 and 1680 cm^{-1}, 1480–1570 cm^{-1} and 1235–1300 cm^{-1}, respectively (Kitagawa and Hirota, 2006). The amide I bonds were seen at 1663 cm^{-1} (Bonifacio et al., 2010). The amide II band is generally weak in Raman spectra, but the amide III band is often more apparent (Jakubek et al., 2017). As shown in Fig. 1D, amide II and amide III bonds were seen at 1542 and 1323 cm^{-1}, respectively (Lippert et al., 1976; Williams, 1986). In a similar way, Amide III band (1200 cm^{-1}–1300 cm^{-1}) which arises from C–N stretching coupled with N–H bending vibrations can give exact information about the protein backbone.

Further characterization on the surfaces of bare ITO electrode and polymer P-PHP immobilized ITO electrode were examined by Energy Dispersive X-Ray (SEM-EDX) to investigate elemental mapping analysis. Fig. SI-5A and 5B inset shows the SEM image of the region was used for mapping. Fig. SI-5A and 5B illustrates the EDX spectrum of the bare ITO and polymer P-PHP film on ITO electrode. The Oxygen(O), Indium(In) and Tin(Sn) signals from the ITO film on PET are clearly observed at 0.5, 3.28 and 3.44 keV, respectively (Fig. SI-5A). (Aydın et al., 2017; Sabouri et al., 2015) When Fig. SI-5B is investigated, EDX-mapping spectra of polymer P-PHP modified ITO includes carbon(C), oxygen(O), Nitrogen(N), Phosphorous(P), Indium(In) and Tin(Sn) elements. The phosphorous and nitrogen signal at 2.01 and 0.38 keV attributed to poly (phosphazene) shell. This analysis shows that the phosphorous and nitrogen atoms in polymer P-PHP backbone was distributed uniformly on the electrode surface, indicating coating P-PHP on ITO surface. When compared Figure. SI-5A was compared to Figure. SI-5B, it was seen that phosphorous and nitrogen containing film was formed on the

ITO electrode surface. The EDX mapping results were also utilized to prove the immobilization of polymer P-PHP onto the ITO electrode surface.

3.2. Electrochemical characterization of the immunosensor

Electrochemical Impedance Spectroscopy (EIS) is a powerful diagnostic tool to investigate the interface features of the modified electrode (Mollarasouli et al., 2018; Wang et al., 2014). Fig. 1E represents the Nyquist plots of different steps in biosensor construction procedure. The EIS data were fitted to a Randles equivalent circuit (inset in Fig. 1E), which contains the electrolyte solution resistance (R_s), the charge transfer resistance (R_{ct}), the constant phase element (CPE) and Warburg impedance to mass transfer (W). In the Nyquist plots, the diameter of the semicircle corresponds to the R_{ct} value of redox conversion of the electroactive probe $[Fe(CN)_6]^{3-/4-}$ on the electrode at certain potential (Chen et al., 2011).

The different stages in the construction of the anti-CDH22/ITO immunosensor were investigated by using EIS and CV. Figs. 1E and 1F show the EIS and CVs recorded for ITO/P-PHP, ITO/P-PHP/anti-CDH 22, ITO/P-PHP/anti-CDH22/BSA, ITO/P-PHP/anti-CDH 22/BSA/CDH22 in 5 mM ferri-ferro solution prepared in 1 M KCl. As it can be seen in Fig. 1E, Nyquist plot with large diameter was obtained after polymer modification. A significant decrease was seen in the charge transfer resistance (R_{ct}), when anti-CDH22 antibodies were immobilized on the modified ITO electrode surface. Additionally, as expected, an increase in the R_{ct} was monitored after BSA blockage. The cause of this increase was aldehyde ends blockage by BSA. When the CDH22 antigens were immobilized on the ITO electrode, the value of R_{ct} increased due to specific reactions between anti-CDH22 antibodies and CDH22 antigens.

Cyclic voltammetry was employed to investigate the various electrochemical characteristics of the redox probe on the modified ITO electrode. Fig. 1F displays the CVs of the same electrodes. As expected, the results of CV measurements are in agreement with those obtained by EIS. Polymer modified ITO electrode had small peak currents due to the non-conductivity of polymer. After antibody immobilization, the peak currents increased. A decrease was seen in the peak currents after BSA blockage step. Finally, when the CDH22 antigens immobilized onto ITO electrode, the peak currents decreased as a consequence of specific interaction between antibody and antigen. In this step, a blocking layer formed and the conductivity of the ITO electrode decreased.

3.3. Surface characterization of the proposed Immunosensor

Surface characterization of the suggested immunosensor was performed using SEM and AFM. Figs. 2A and 2B show bare ITO electrode surface obtained by SEM and AFM. The electrode surface was smooth and pure and the average roughness (Ra) of this surface was found as 4.5 nm. After the film formation with spin-coating method (Figs. 2C and 2D), the surface image was changed and polymer distributed homogenously on the electrode surface and looked like spherical grains. This smooth surface was slightly roughened after polymer modification and the Ra value was measured as 202.6 nm. These spherical grains showed densely porosity, which created a uniformly modified ITO electrode surface for immobilization of CDH22 antibody. Figs. 2E and 2F show the effective immobilization of anti-CDH22 antibodies. As seen in Fig. 2E, antibodies are found on the electrode surface and looked like granules. The Ra value of this surface was found as 42.5 nm. In this study, BSA was utilized as blockage agent and it looked like layers (Figs. 2G and 2H). After BSA blockage, the Ra value was found as 33.7 nm. After specific interaction between antibody and antigen, the electrode surface was changed (Figs. 2I and 2J). The Ra value was measured as 43.9 nm. The change at surface proved the successful interaction.

3.4. Optimization of the experimental parameters in the fabrication of the immunosensor

The different parameters affecting the fabrication of immunoelectrode and the success of the proposed immunosensor were evaluated.

The first optimization step was the determination of polymer concentration. Three different amounts (0.1 mg/mL, 0.25 mg/mL, 0.5 mg/mL) of polymer were used to achieve maximum immunosensor signal. An increase in the amount of polymer caused a decrease in the immunosensor signal. This decrease was originated from the extreme abundance of aldehyde group formation. Therefore 0.1 mg/mL was selected as optimum level in biosensor fabrication (Fig. 3A). Another optimization step was to optimize antibody concentration immobilized on the ITO electrode. This stage is significant because antibodies on the electrode surface bind to CDH22 antigen within the sample. Therefore, 3 different antibody concentrations were utilized. At low antibody level, a low signal was obtained since a small amount of antibodies captured a small amount of antigens. Maximum signal was attained at 5 ng/mL antibody concentration. When 2 ng/mL antibodies were utilized, the signal had similar signal with 5 ng/mL antibody usage. For this reason, 2 ng/mL was selected as optimal concentration (Fig. 3B). Antibody incubation time is important in immunosensor response level. The signal at 30 min was very low, which illustrated that bounded antibody amount was not enough for antigen detection. The signals at 45 and 60 min were similar. Because of this 45 min was selected as optimal one (Fig. 3C). To optimize antigen incubation time, different durations (30 min, 45 min, 60 min) were used as incubation time. The responses in these durations were similar. Because of this, maximum response was obtained at 30 min (Fig. 3D). These optimized variables were utilized in further experiments to obtain wide detection range. The statistical test illustrated that the results of concentration optimization studies (polymer and antibody concentration optimization) were not statistically meaningful because $p = 0.136$ and 0.209 values found with T test were higher than 0.05. And the results of incubation time optimization studies (antibody and antigen concentration optimization) were statistically meaningful because $p = 0.035$ value found with T test was lower than 0.05. ANOVA test was performed to determine whether the groups were different. And the effect of the optimization parameters on the immunosensor response were investigated ANOVA test. The results of polymer concentration, antibody concentration, antibody and antigen incubation time were evaluated separately. P values of these parameters were low than 0.01 and the effect of these parameters on the immunosensor response were found as meaningful.

3.5. Analytical characteristics for the determination of CDH22

Under the optimized experimental conditions, a linear increase pattern was seen in impedance values with increasing CDH22 concentrations. The cause of gradual increase was a gradual increase in non-conductivity property of antigen layer on ITO electrode surface (Fig. 4A). Also, specific interaction between antibody and antigen formed a complex and a physical barrier that causes an increase in electron transfer resistance and a decrease in the peak currents (Fig. 4B). In other words, the specific antibody CDH22 antigen recognition interaction induced a decrease in the electron transfer, which corresponds to the different concentrations of CDH22. The detection range of CDH22 immunosensor was calculated by using EIS datas and it exhibited good detection range for CDH22 with excellent linearity (0.015–2.9 mL) (Fig. 4C). According to the 3 sb and 10 sb rule, where sb was calculated as the standard deviation ($n = 10$) for measurements in the absence of CDH22, detection (LOD) and quantification (LOQ) limits of 4.4 fg/mL and 15 fg/mL respectively.

In this study, SFI technique was utilized for monitoring of impedance-based CDH22 immunosensor behaviour. To monitor antibody and antigen interaction, impedance was measured at constant

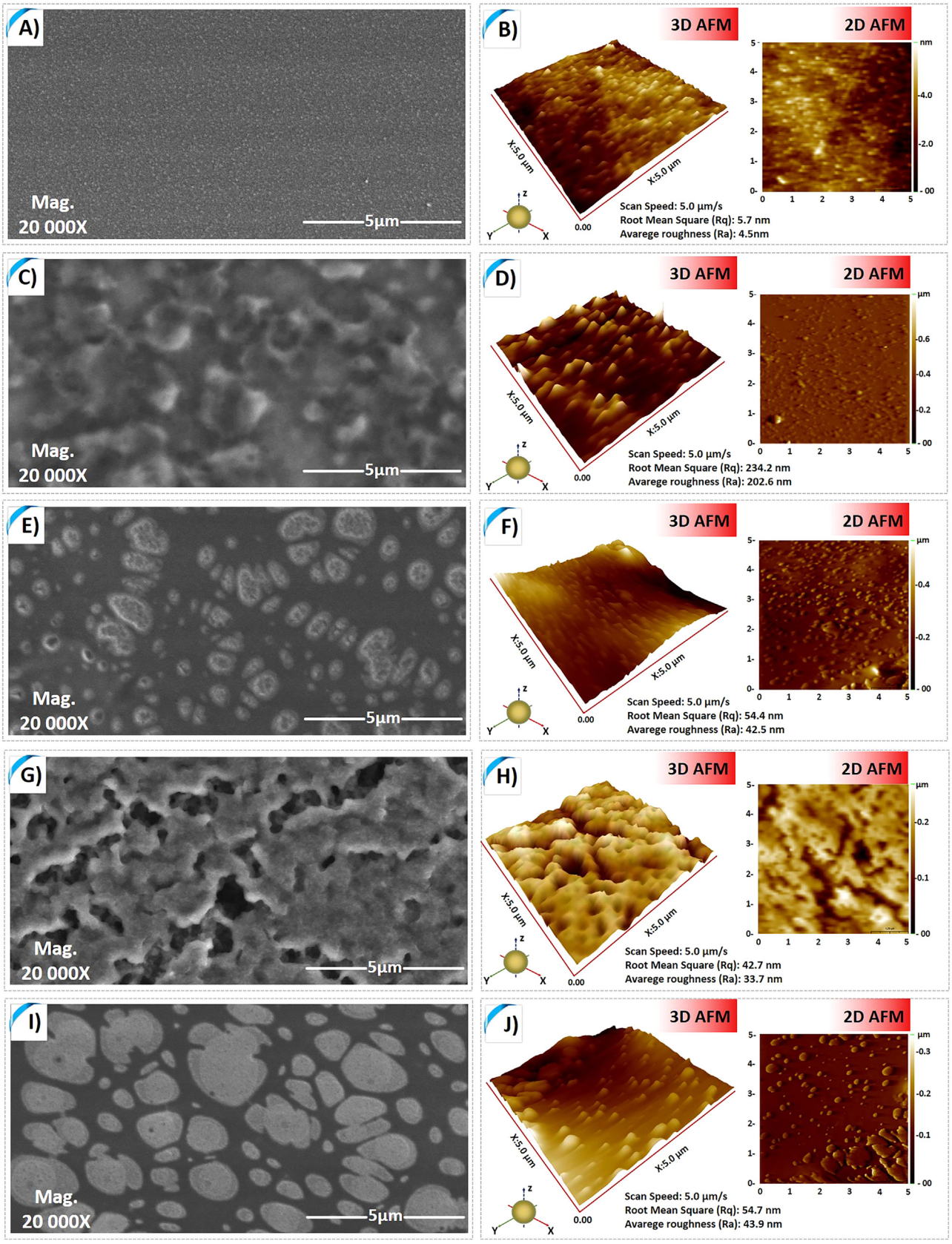

Fig. 2. SEM and AFM images of different immobilization stages.

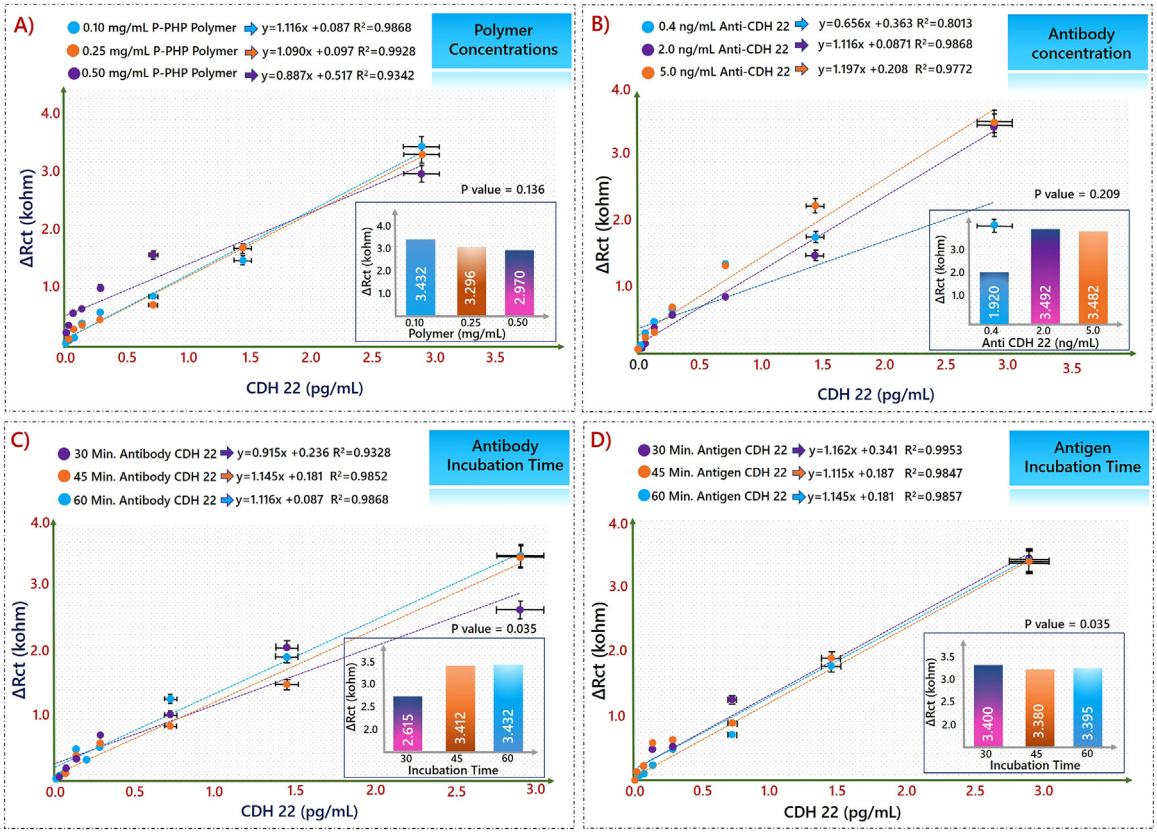

Fig. 3. Optimization studies (A) P-PHP concentration, (B) anti-CDH 22 concentration, (C) anti-CDH 22 incubation time, (D) CDH 22 antigen incubation time.

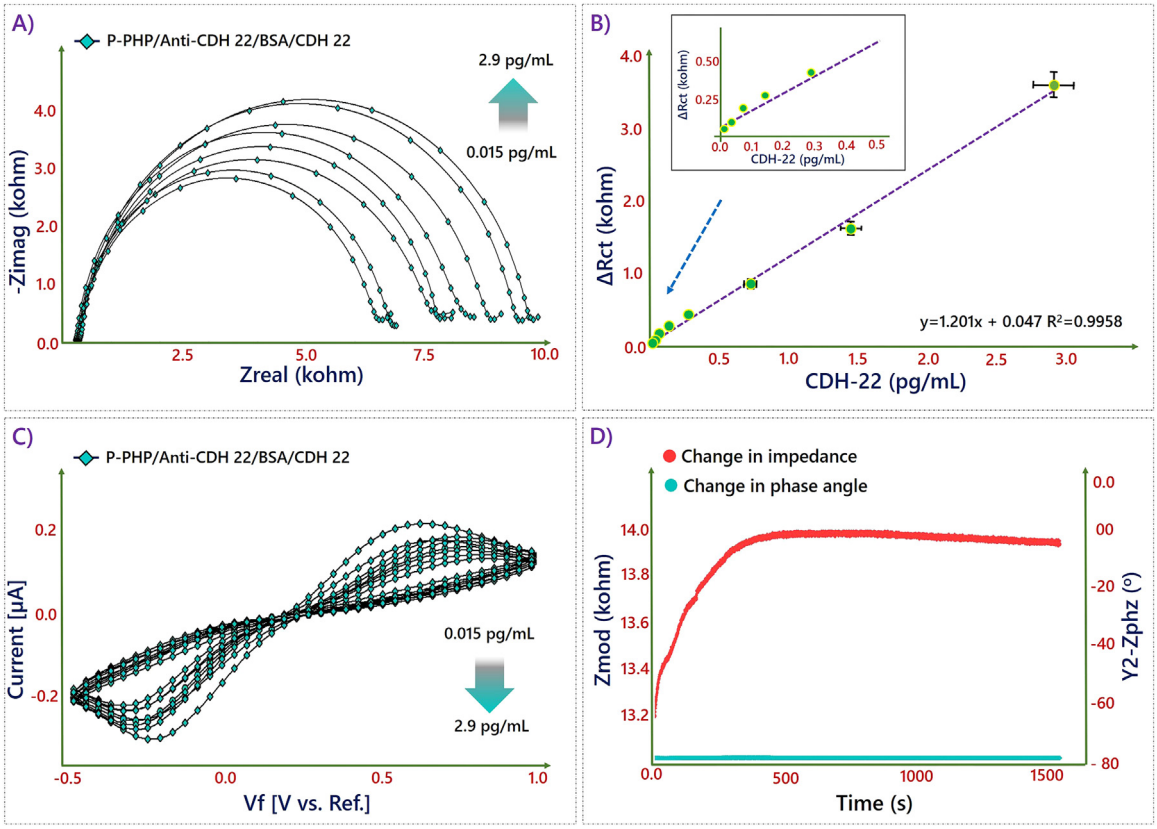

Fig. 4. EIS (A) and CV (B) responses of the immunosensor for the detection of CDH22 antigen (from 0.015 to 2.9 pg/mL), calibration curve (C), Single frequency impedance (D).

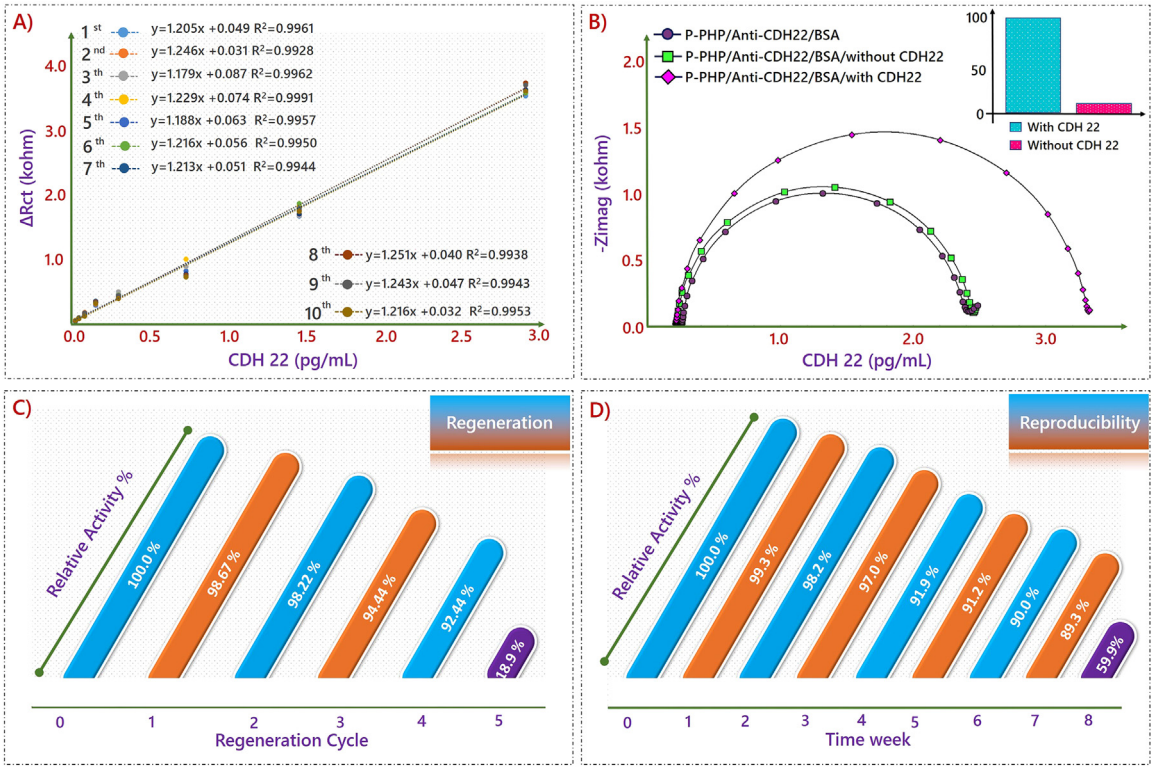

Fig. 5. Reproducibility (A), selectivity (B), regeneration (C) and Storage stability (D) of the Immunosensor.

frequency that was chosen by using Bode plot as 20 Hz (Fig. SI-6). The SFI measurement was taken in PBS buffer (pH 7.4). As seen in Fig. 4D, an increase was observed after antigen addition in electrochemical cell including PBS buffer.

3.6. Repeatability, reproducibility, storage stability and selectivity of the fabricated immunosensor

The repeatability of the measurements was evaluated by measuring 0.35 pg/mL CDH22 standard solution with 20 different immune-electrodes fabricated under the same conditions. A relative standard deviation (RSD) value of 5.14% was calculated and this value indicated an acceptable repeatability for both the procedures utilized in the immunosensor fabrication and the impedimetric measurements. To investigate reproducibility, 10 different immunosensors were fabricated on the same day and in the same manner. RSD of 10 different immunosensors was calculated as 1.99% (Fig. 5A).

The selectivity of the biosensor was monitored by comparing impedance signal in the presence and absence of CDH22 in PBS solution. For the selectivity test, non-target proteins such as IL-1α, IL-1β, IL-8, TNF-α, Sox2 and Rack1 were utilized at high concentration. Fig. 5B illustrates that no significant differences were seen in impedance value in the presence of interference proteins, confirming the good selectivity of the biosensor.

Regeneration of an immunosensor is important to reduce costs and accelerate the commercialization process. Therefore, regeneration studies were performed. Anti-CDH22 antibody immobilized ITO electrode was dipped in PBS solution containing CDH22 antigen. Then, the impedance value was recorded. After that, it was dipped in a HCl solution (10 mM, 5 min). During this process the specific bonds between antibody and antigen were broke down. Following this, the regenerated electrode surface was dipped in PBS solution including CDH22 antigen (0.35 pg/mL). After 4 regeneration stages, immunosensor had good response. However, after 5 regeration stage the electrode surface was damaged and it had low activity (Fig. 5C).

The storage stability of the constructed immunosensor was evaluated by storing at 4 °C. Different immunoelectrodes were constructed on the same day, stored at 4 °C in a dry environment and utilized on different days for measurement of 0.35 pg/mL standard CDH22 solution. Storage test results illustrated that the signal of the immunosensor decreased 60% after 8 weeks of storage, thereby suggesting an acceptable eight-week storage stability of the fabricated immunosensor (Fig. 5D).

3.7. Determination of CDH22 in human serum

The practical applicability of the biosensor was examined by determination of CDH22 in human serum samples obtained from the NKU hospital. The accuracy of the fabricated immunosensor was investigated by using standard addition method. As seen in the obtained results, there was no apparent matrix effect when human serum samples were 10,000 times diluted (Table SI-1).

4. Conclusion

In this study, we fabricated a reusable and sensitive immunosensor to detect CDH22 cancer biomarker. In this design, benzaldehyde substituted poly(phoshozene) polymer was used as antibody immobilization matrix. Anti-CDH22 antibodies were bound to aldehyde groups of polymer covalently and provided a specific affinity interaction between CDH22 antigens. EIS technique was utilized for quantitative determination of CDH 22 antigens. Apart from this technique, CV was utilized to monitor electrode modification steps and SFI was utilized to prove anti-CDH22 antibody-CDH22 antigen interaction. Morphological characterization of the fabrication steps of the immunosensor was carried out with SEM and AFM measurements. The formed film on the ITO electrode and antibody immobilization was investigated by using FTIR and RAMAN spectroscopy. The fabricated immunosensor showed a very good analytical performance in terms of sensitivity, selectivity and stability. In addition, the electrode can be conveniently reused for the

next detection. This immunosensor had a wide range (0.015–2.9 pg/mL) and low LOD (4.4 fg/mL). Moreover, the analyses of human serum samples required simple sample dilution with PBS and had good recovery (96.46–100.82%). Also, the suggested immunosensor was successful for CDH22 detection in human serum and aldehyde polymer was a suitable platform for anti-CDH22 antibody immobilization. We hope that the proposed immunosensor will lead to improving the fabrication of biosensor based on polymer. In addition, the proposed immunosensor can serve as an attractive candidate for other conventional methods such as ELISA and radio immunoassay. This novel benzaldehyde substituted poly(phoshozene) polymer coated electrochemical immunosensor provides a simple, inexpensive and rapid analytical strategy to detect CDH22 biomarker in human serum samples, which offers a promising strategy for quantification of CDH22 biomarker with minimized sample preparation steps. Moreover, the immunosensor may open new ways for the point-of-care detection of biomarkers.

Acknowledgment

The financial support from TÜBITAK (The Scientific and Technological Research Council of Turkey) (Grant no.113 Z 678) is gratefully acknowledged.

Appendix A. Supporting information

Supplementary data associated with this article can be found in the online version at doi:10.1016/j.bios.2018.10.051

References

Allcock, H.R., 1998. Appl. Organomet. Chem. 12 (10-11), 659–666.
Allcock, H., Kugel, R., Valan, K., 1966. Inorg. Chem. 5 (10), 1709–1715.
Allcock, H.R., 1992. J. Inorg. Organomet. Polym. 2 (2), 197–211.
Alula, M.T., Mengesha, Z.T., Mwenesongole, E., 2018. Vib. Spectrosc. 98, 50–63.
Amani, J., Maleki, M., Khoshroo, A., Sobhani-Nasab, A., Rahimi-Nasrabadi, M., 2018. Anal. Biochem. 548, 53–59.
Arya, S., Estrela, P., 2018. Sensors 18 (7), 2010.
Aydın, E.B., Aydın, M., Sezgintürk, M.K., 2017. Biosens. Bioelectron. 97, 169–176.
Aydın, E.B., Aydın, M., Sezgintürk, M.K., 2018a. Sens. Actuators B 270, 18–27.
Aydın, E.B., Sezgintürk, M.K., 2017. Trends Anal. Chem. 97, 309–315.
Aydın, E.B., Sezgintürk, M.K., 2018. Anal. Chim. Acta. https://doi.org/10.1016/j.aca.2018.07.055.
Aydın, M., Aydın, E.B., Sezgintürk, M.K., 2018a. Biosens. Bioelectron. 107, 1–9.
Aydın, M., Aydın, E.B., Sezgintürk, M.K., 2018b. Biosens. Bioelectron. 117, 720–728.
Bahadır, E.B., Sezgintürk, M.K., 2015. Talanta 132, 162–174.
Banas, A., Banas, K., Furgal-Borzych, A., Kwiatek, W., Pawlicki, B., Breese, M., 2015. Analyst 140 (7), 2156–2163.
Bojorge Ramírez, N., Salgado, A., Valdman, B., 2009. Braz. J. Chem. Eng. 26 (2), 227–249.
Bonifacio, A., Beleites, C., Vittur, F., Marsich, E., Semeraro, S., Paoletti, S., Sergo, V., 2010. Analyst 135 (12), 3193–3204.
Carriedo, G.A., García Alonso, F.J., González, P.A., Menéndez, J.R., 1998. J. Raman Spectrosc. 29 (4), 327–330.
Chen, M., Lord, R., 1974. J. Am. Chem. Soc. 96 (15), 4750–4752.
Chen, Y., Jiang, B., Xiang, Y., Chai, Y., Yuan, R., 2011. Chem. Commun. 47 (48), 12798–12800.
Ferreira, N.S., Sales, M.G.F., 2014. Biosens. Bioelectron. 53, 193–199.
Fiedler, C., Luerssen, B., Lucht, B., Janek, J., 2018. J. Power Sources 384, 165–171.
Ghayedi Karimi, K., Mozaffari, S.A., Ebrahimi, M., 2018. J. Chin. Chem. Soc. 1–10.
Jakubek, R.S., Handen, J., White, S.E., Asher, S.A., Lednev, I.K., 2017. TrAC Trends Anal. Chem. 103, 223–229.
Jiang, P., Gu, X., Zhang, S., Sun, J., Xu, R., Bourbigot, S., Duquesne, S., Casetta, M., 2015. Polymer 79, 221–231.
Karimi, F., Shojaei, A.F., Tabatabaeian, K., Karimi-Maleh, H., Shakeri, S., 2017. IET Nanobiotechnol. 12 (3), 336–342.
Karimi-Maleh, H., Biparva, P., Hatami, M., 2013. Biosens. Bioelectron. 48, 270–275.
Karimi-Maleh, H., Tahernejad-Javazmi, F., Ensafi, A.A., Moradi, R., Mallakpour, S., Beitollahi, H., 2014. Biosens. Bioelectron. 60, 1–7.
Kelly, N., Varga, J., Specker, E., Romeo, C., Coomber, B., Uniacke, J., 2018. Oncogene 37 (5), 651.
Khashayar, P., Amoabediny, G., Larijani, B., Hosseini, M., Vanfleteren, J., 2017. Sci. Rep. 7 (1), 16070.
Kitagawa, T., Hirota, S., 2006. New York: Wiley.
Kumar, S., Singh, R.K., Murthy, R., Bhardwaj, T., 2015. Pharm. Res. 32 (8), 2736–2752.
Lippert, J., Tyminski, D., Desmeules, P., 1976. J. Am. Chem. Soc. 98 (22), 7075–7080.
Luther, T.A., Stewart, F.F., Budzien, J.L., LaViolette, R.A., Bauer, W.F., Harrup, M.K., Allen, C.W., Elayan, A., 2003. J. Phys. Chem. B 107 (14), 3168–3176.
Martín-Sánchez, E., Mendaza, S., Ulazia-Garmendia, A., Monreal-Santesteban, I., Córdoba, A., Vicente-García, F., Blanco-Luquin, I., De La Cruz, S., Aramendia, A., Guerrero-Setas, D., 2017. Clin. Epigenet. 9 (1), 7.
Mollarasouli, F., Serafín, V., Campuzano, S., Yáñez-Sedeño, P., Pingarrón, J.M., Asadpour-Zeynali, K., 2018. Anal. Chim. Acta 1011, 28–34.
Pamukçi, O., Çil, E., Begeç, S., Arslan, M., 2007. Heteroat. Chem. 18 (7), 791–797.
Piche, B., Khosravi, S., Martinka, M., Ho, V., Li, G., 2011. Am. J. Cancer Res. 1 (2), 233.
Rauf, S., Mishra, G.K., Azhar, J., Mishra, R.K., Goud, K.Y., Nawaz, M.A.H., Marty, J.L., Hayat, A., 2018. Anal. Biochem. 545, 13–19.
Sabouri, H., Ohno, K., Perrier, S., 2015. Polym. Chem. 6 (41), 7297–7307.
Sohn, Y.S., Cho, Y.H., Baek, H., Jung, O.-S., 1995. Macromolecules 28 (22), 7566–7568.
Tranter, G., 2017. Elsevier, pp. 740–758.
Sohn, Y., Jun, Y., 2009. Polyphosphazenes for Biomedical Applications. Poly-and Cyclotriphosphazenes as Drug Carriers for Anticancer Therapy. A John Wiley & Sons, New Jersey, pp. 249–275.
Wang, H.-B., Zhang, H.-D., Xu, S.-P., Gan, T., Huang, K.-J., Liu, Y.-M., 2014. Sens. Actuators B: Chem. 194, 478–483.
Williams, R.W., 1986. Methods Enzymol. 311–331.
Zhou, J., Li, J., Chen, J., Liu, Y., Gao, W., Ding, Y., 2009. Tumor Biol. 30 (3), 130–140.
Zhou, C., Liu, D., Xu, L., Li, Q., Song, J., Xu, S., Xing, R., Song, H., 2015. Sci. Rep. 5, 9939.